

Cite this: *J. Mater. Chem.*, 2012, **22**, 11452

www.rsc.org/materials

Facile and effective synthesis of reduced graphene oxide encapsulated sulfur via oil/water system for high performance lithium sulfur cells†Fei-fei Zhang,^{ab} Xin-bo Zhang,^{*a} Yun-hui Dong^b and Li-min Wang^{*a}

Received 12th December 2011, Accepted 1st May 2012

DOI: 10.1039/c2jm16543k

A novel sulfur@rGO composite material with a sacculle-like structure is synthesized via a facile and effective strategy with an oil in water (O/W) system. The obtained materials exert outstanding electrochemical performance at high rates as a cathode material for rechargeable lithium sulfur cells.

Following two decades of intensive exploration, lithium-ion batteries (LIBs) have achieved great commercial success among the energy storage systems.¹ However, the capacities of current cathode materials, such as transition metal oxides and phosphates, have reached their limits, which are too low to meet the requirements for emerging large-scale energy storage applications.² In this context, the lithium-sulfur (Li-S) cell has been envisaged as a promising candidate due to its high theoretical capacity (1675 mA h g⁻¹, only lower than the O₂ cathode), high specific energy density (2500 W h kg⁻¹ or 2800 W h L⁻¹), abundant resources, low cost, and nontoxicity.³ However, the use of sulfur as the desired cathode material also needs to overcome many challenges. Typically, sulfur and sulfur-containing organic compounds are highly electrically and ionically insulating, which results in the low utilization of sulfur and low columbic efficiency.⁴ Another major hurdle is the serious capacity degradation upon cycling due to the solubility of the electrochemical reaction products of polysulfides (Li₂S_x, 4 ≤ x ≤ 8) in the electrolyte, reactions between polysulfides and lithium negative electrodes, and large volumetric expansion of sulfur (~80%) during cycling.⁵ To solve these problems, carbon-based materials with small pore size and large pore volume, such as mesoporous carbon, carbon nanofiber, carbon nanotube, hollow carbon and so on, have proved their efficacy in enhancing the conductivity and retaining polysulfides, therefore improving the performance of Li-S cells.⁶

Graphene, as a single-atom-thick carbon material, inherently holds many favorable advantages such as extremely high surface area, extraordinary thermal/electrical conductivity, light weight, excellent flexibility and mechanical strength, *etc.*, and thus is expected to find

exciting application in electronics, engineering materials, and as an ideal substrate for electrochemical energy storage applications.⁷ It was reported that a sulfur-graphene composite was synthesized by using physical vapor deposition method,^{7b} in which the graphene could improve the conductivity of sulfur, but the two-dimensional (2D) structure was not effective in containing the polysulfides. In a recent report, a two-step method is provided, in which poly-(ethyleneglycol)-containing surfactant coated sulfur particles are synthesized and wrapped by carbon black decorated graphene oxide sheets.^{7c} The graphene-sulfur composite showed high specific capacity with relatively good cycling stability as the cathode for Li-S cells. Despite this progress, direct accommodation of sulfur by graphene with particular structure designs and method innovation, until now, has been rarely reported.

Herein, sulfur encapsulated by reduced graphene oxide (S@rGO) with sacculle-like subunits is synthesized by a facile quasisemulsion-templated method in an O/W system. The sulfur nanoparticles can distribute homogeneously in the microreactor. When tested as anode materials for Li-S cells, the unique sacculle-like structure and sulfur nano-particles display a remarkable improvement in the high rate performances.

The detailed synthetic procedures are shown in Fig. 1. Typically, graphene oxide (GO) is first dispersed with water to form a homogeneous suspension (water-phase) under ultrasonic conditions. Then the oil-phase containing sulfur in carbon disulfide (CS₂) is added dropwise into the GO solution under ultrasonication. Following complete evaporation of CS₂ from the mixture, hydrazine hydrate (N₂H₄·H₂O) is then added to reduce GO to rGO. After stirring for 12 hours at room temperature, the S@rGO composite is collected by consecutive centrifugation and water-washing cycles as well as lyophilization.

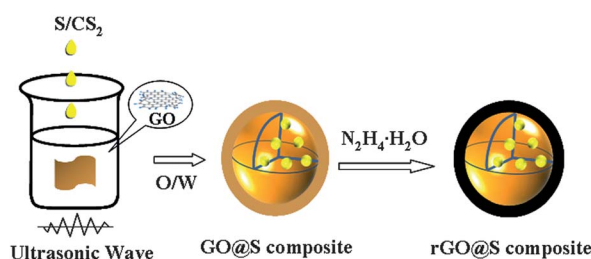


Fig. 1 Schematic of synthesis steps for S@rGO composite.

^aState Key Laboratory of Rare Earth Resource Utilization, Changchun Institute of Applied Chemistry, Chinese Academy of Sciences, Changchun 130022, Jilin, China. E-mail: xbzhang@ciac.jl.cn; lmwang@ciac.jl.cn

^bSchool of Chemical Engineering, Shandong University of Technology, Zibo 255091, China

† Electronic supplementary information (ESI) available. See DOI: 10.1039/c2jm16543k

The microstructures of the as-synthesized sample are characterized by scanning electron microscopy (SEM). The dimension of the composite particles before reduction is *ca.* 1 μm (Fig. S1a†). The image shows GO sheets coating the particles, indicating the feasibility of our strategy in preparing an encapsulated structure using an O/W system. Interestingly, after reduction with $\text{N}_2\text{H}_4 \cdot \text{H}_2\text{O}$, the size and surface morphology of the composite particles remains almost unchanged (Fig. 2a). The relative change in the ratio of D to G peak intensity in the Raman spectra before and after the reduction confirms the reduction of GO (Fig. S2†).⁸ Transmission electron microscopy (TEM) is also applied to analyze the morphology and structure of the interior sulfur (Fig. 2c). Unexpectedly, the interior sulfur encapsulated by rGO is not composed of a large particle but many smaller ones with sizes ranging from 10 to 100 nm. This is reasonable when considering the peculiarity of the proposed synthetic process. The oil droplets of CS_2 containing sulfur are first split into smaller droplets and surrounded by GO sheets under ultrasonic conditions. Then, due to the volatile nature of CS_2 , it gradually evaporated from the O/W system accompanied by the formation of the saccule-like structure, and causing the dissolving sulfur to recrystallize into smaller particles. Furthermore, the generated sulfur particles are basically adsorbed onto rGO with the aid of functional groups on the surface of rGO, which is confirmed by the high resolution TEM image (Fig. 2d). It should be noted that the obtained saccule-like structure has enough space to accommodate volumetric expansion of sulfur during charge–discharge process.

To further verify the structure and composition of the S@rGO composite, energy dispersive spectrometer (EDS) mapping of the material is carried out (Fig. S3†). The corresponding element mapping of sulfur, carbon and oxygen clearly shows that sulfur is encapsulated by GO in the saccule-like structure, which is consistent with the results of the SEM and TEM images. X-ray diffraction (XRD) analyses are also conducted on the obtained S@rGO composite and elemental sulfur (Fig. S4†). The reflections of the elemental sulfur showed two prominent peaks at $2\theta = 23$ and 28° , corresponding to an *Fddd* orthorhombic structure.^{3a,9} Compared with the pattern of the elemental sulfur, the characteristic peaks in the

XRD pattern of the S@rGO composite remain the same, further indicating the existence of sulfur in the saccule-like structure. Elemental analysis determines that the content of sulfur in the S@rGO is as high as 65 wt% (Table 1).

To evaluate the electrochemical performance of the S@rGO composite, coin cells are fabricated with lithium foil as the anode. The electrolyte is 1 M of lithium bis(trifluoromethanesulfonyl)imide (LiTFSI) in 1,3-dioxolane and 1,2-dimethoxyethane (volume ratio 1 : 1). Fig. 3a shows the first cycle charge and discharge curves of the composite material at various high rates between 1.2 and 3.0 V. The discharge capacity is $724.5 \text{ mA h g}^{-1}$ (all the specific capacities in this article are calculated based on the sulfur mass only) at a current rate of 1C ($1\text{C} = 1675 \text{ mA g}^{-1}$). The discharge capacity remains as high as 715.6, 708.6 and $697.5 \text{ mA h g}^{-1}$ at 2C, 3C and 4C, respectively, which are unprecedented results for Li–S cells at these high rates. The performance is much better than the S–rGO cathode as shown as Fig. S6a.† All the discharge curves show typical two plateaus, corresponding to the reduction of elemental S to higher-order Li polysulfides (Li_2S_n , $2 \leq n \leq 8$) and lower-order Li sulfides (Li_2S_2 or Li_2S), while the charge process due to oxidation appears relatively similar.^{3a,6d,10} The electrochemical reactions of the cathode can be more clearly indicated in the cyclic voltammetry (CV) profile (Fig. S5†). The measurement is conducted between 1.0 and 3.0 V at a scan speed of 0.1 mV s^{-1} . During the first cathodic scan, two main reduction peaks at around 2.4 and 2.0 V are clearly shown, suggesting a two-step reduction of sulfur. In the subsequent anodic scan, only one intensive oxidation peak is observed at about 2.5 V which is attributed to the conversion of Li_2S and polysulfides into elemental S.

The cycling performance of the Li–S cell is shown in Fig. 3b. It is seen that the discharge capacity increases gradually with increasing cycle number during the first several cycles. This could be explained by considering that the S@rGO composite in the cathodes is incompletely soaking in and penetrated by the electrolyte, which is due to the preparation process of the cathodes. As the reaction proceeds, more and more sulfur particles in the relatively closed structure are exposed to the electrolyte. The coulombic efficiency is higher than 100% at the first cycles (Fig. S8†). At a rate of 1C, the cathode retains the reversible discharge specific capacity of $621.9 \text{ mA h g}^{-1}$ at the 60th cycle. Good retention with capacity (85.8%) and high coulombic efficiency (>95%) reflect the good cycling stability of the S@rGO composite cathode. At the high rates of 2C, 3C and 4C, the capacities remain at 530.8, 505.8 and $478.7 \text{ mA h g}^{-1}$ at the 60th cycle, respectively, and the 60th charge–discharge profiles also reveal the good performance of the cells (Fig. S7†). In contrast, the discharge specific capacity of the S–rGO cathode is low at a rate of 1C, and there are no effectively reversible reactions carried out at higher rates (Fig. S6b†). As the electrochemical impedance response (EIS) measurements in Fig. S9† show, the S–rGO cathode shows higher charge-transfer resistance than the S@rGO cathode. The saccule-like structure of rGO can provide a more effective electronically conductive network than common rGO sheets. Furthermore, the good cycling stability of the cathode at high rates is due to the

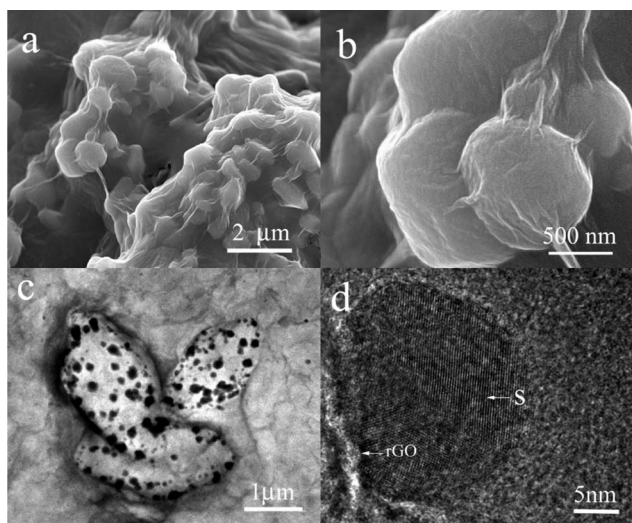


Fig. 2 (a) and (b) SEM, (c) TEM, and (d) HRTEM images of the S@rGO composite.

Table 1 Elemental analysis of the S@rGO composite

Element	N	C	H	S
Weight%	1.36	24.69	0.736	64.96

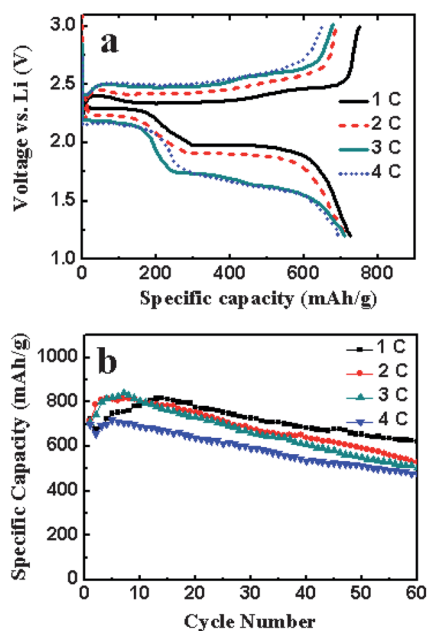


Fig. 3 (a) First cycle charge–discharge voltage profiles of the S@rGO cathodes at various C rates. (b) Cycle performance of the S@rGO cathodes at various C rates.

excellent flexibility and mechanical strength of graphene. The unique saccule-like structure of the composite could provide enough space to accommodate stress and volumetric expansion of sulfur during the charge–discharge process. The functional groups on the rGO surface can improve the overall electrochemical performance of the composite cathode. Firstly, the functional groups on the rGO surface inside the saccule can provide cushioning space during the discharge process. Secondly, these functional groups on the rGO saccule can have an adsorbing ability to anchor S atoms and to partially prevent the polysulfides from dissolving in the electrolyte during cycling.^{7d} However, the problem of polysulfide dissolution has not been solved completely, as there is some capacity loss in the cycling process. Further endeavor is needed to solve this problem.

In summary, we have developed a facile and effective methodology to encapsulate sulfur by rGO with an O/W system for the large-scale synthesis of S@rGO composites. When tested as the cathode material in a Li–S secondary cell, the as-prepared S@rGO composite exhibited outstanding electrochemical features at high rates, deriving from the fact that such a unique saccule-like structure of rGO gave the sulfur particles electrical conductivity, prevented the polysulfides from dissolving in the electrolyte effectively during cycling and accommodated the stress and volume expansion during discharge. In addition, the strategy for preparing saccule-like structures can

certainly be extended to synthesize other functional materials in many fields.

Acknowledgements

This work is financially supported by 100 Talents Programme of The Chinese Academy of Sciences, Foundation for Innovative Research Groups of the National Natural Science Foundation of China (no. 20921002), National Natural Science Foundation of China (Grant no. 21101147), and the Jilin Province Science and Technology Development Program (Grant no. 20100102 and 20116008).

Notes and references

- P. G. Bruce, L. J. Hardwick and K. M. Abraham, *MRS Bull.*, 2011, **36**, 506.
- (a) X. Ji and L. Nazar, *J. Mater. Chem.*, 2010, **20**, 9821; (b) J. M. Tarascon and M. Armand, *Nature*, 2001, **414**, 359.
- (a) X. Ji, K. Lee and L. Nazar, *Nat. Mater.*, 2009, **8**, 500; (b) L. C. Yin, J. L. Wang, J. Yang and Y. Nuli, *J. Mater. Chem.*, 2011, **21**, 6807; (c) L. Ji, M. Rao, S. Aloni, L. Wang, E. J. Cairns and Y. Zhang, *Energy Environ. Sci.*, 2011, **4**, 5053.
- (a) D. Marmorstein, T. H. Yu, K. A. Striebel, F. R. McLarnon, J. Hou and E. J. Cairns, *J. Power Sources*, 2000, **89**, 219; (b) H. Yamin and E. Peled, *J. Power Sources*, 1983, **9**, 281.
- (a) H. Yamin, A. Gorenshtein, J. Penciner, Y. Stenberg and E. Peled, *J. Electrochem. Soc.*, 1988, **135**, 1045; (b) A. Evans, M. I. Montenegro and D. Pletcher, *Electrochem. Commun.*, 2001, **3**, 514; (c) S. E. Cheon, S. S. Choi, J. S. Han, Y. S. Choi, B. H. Jung and H. S. Lim, *J. Electrochem. Soc.*, 2004, **151**, A2067; (d) R. D. Rauh, F. S. Shuker, J. M. Marston and S. B. Brummer, *J. Inorg. Nucl. Chem.*, 1977, **39**, 1761; (e) G. Jeong, Y.-U. Kim, H. Kim, Y.-J. Kim and H.-J. Sohn, *Energy Environ. Sci.*, 2011, **4**, 1986.
- (a) S. R. Chen, Y. P. Zhai, G. L. Xu, Y. X. Jiang, D. Y. Zhao, J. T. Li, L. Huang and S. G. Sun, *Electrochim. Acta*, 2011, **56**, 9549; (b) G. Zheng, Y. Yang, J. J. Cha, S. S. Hong and Y. Cui, *Nano Lett.*, 2011, **11**, 4462; (c) W. Wei, J. Wang, L. Zhou, J. Yang, B. Schumann and Y. NuLi, *Electrochem. Commun.*, 2011, **13**, 399; (d) N. Jayaprakash, J. Shen, S. S. Moganty, A. Corona and L. A. Archer, *Angew. Chem.*, 2011, **123**, 6026; (e) S. Wei, H. Zhang, Y. Huang, W. Wang, Y. Xia and Z. Yu, *Energy Environ. Sci.*, 2011, **4**, 736.
- (a) M. Choucair, P. Thordarson and J. A. Stride, *Nat. Nanotechnol.*, 2009, **4**, 30; (b) J. Z. Wang, L. Lu, M. Choucair, J. A. Stride, X. Xu and H. K. Liu, *J. Power Sources*, 2011, **196**, 7030; (c) H. Wang, Y. Yang, Y. Liang, J. T. Robinson, Y. Li, A. Jackson, Y. Cui and H. Dai, *Nano Lett.*, 2011, **11**, 2644; (d) L. Ji, M. Rao, H. Zheng, L. Zhang, Y. Li, W. Duan, J. Guo, E. J. Cairns and Y. Zhang, *J. Am. Chem. Soc.*, 2011, **133**, 18522; (e) J. Xiao, D. Mei, X. Li, W. Xu, D. Wang, G. L. Graff, W. D. Bennett, Z. Nie, L. V. Saraf, I. A. Aksay, J. Liu and J. G. Zhang, *Nano Lett.*, 2011, **11**, 5071.
- (a) Y. Xu, K. Sheng, C. Li and G. Shi, *J. Mater. Chem.*, 2011, **21**, 7376; (b) H. L. Wang, J. T. Robinson, X. L. Li and H. J. Dai, *J. Am. Chem. Soc.*, 2009, **131**, 9910.
- (a) B. Zhang, X. Qin, G. R. Li and X. P. Gao, *Energy Environ. Sci.*, 2010, **3**, 1531; (b) F. Wu, J. Z. Chen, R. J. Chen, S. X. Wu, L. Li, S. Chen and T. Zhao, *J. Phys. Chem. C*, 2011, **115**, 6057.
- (a) J. Shim, K. A. Striebel and E. J. Cairns, *J. Electrochem. Soc.*, 2002, **149**, A1321; (b) Y. Jung and S. Kim, *Electrochem. Commun.*, 2007, **9**, 249; (c) J. H. Shin and E. J. Cairns, *J. Power Sources*, 2008, **177**, 537.